JOURNAL OF BACTERIOLOGY, June 2011, p. 3020–3032 Vol. 193, No. 12
0021-9193/11/$12.00 doi:10.1128/JB.00017-11
Copyright © 2011, American Society for Microbiology. All Rights Reserved.

An Orphan Histidine Kinase, OhkA, Regulates Both Secondary Metabolism and Morphological Differentiation in *Streptomyces coelicolor*▽†

Yinhua Lu,[1] Juanmei He,[1] Hong Zhu,[1] Zhenyu Yu,[1] Rui Wang,[1] Yunliang Chen,[1] Fujun Dang,[1] Weiwen Zhang,[2] Sheng Yang,[1] and Weihong Jiang[1]*

Key Laboratory of Synthetic Biology, Institute of Plant Physiology and Ecology, Shanghai Institutes for Biological Sciences, Chinese Academy of Sciences, Shanghai 200032, People's Republic of China,[1] and School of Chemical Engineering and Technology, Tianjin University, Tianjin 300072, People's Republic of China[2]

Received 5 January 2011/Accepted 7 April 2011

We report here the physiological and genetic characterization of an orphan histidine kinase (HK) (OhkA, *SCO1596*) in *Streptomyces coelicolor* and its homolog (OhkAsav, *SAV_6741*) in *Streptomyces avermitilis*. The physiological analysis showed that the *ohkA* mutant of *S. coelicolor* exhibits impaired aerial mycelium formation and sporulation and overproduction of multiple antibiotics on mannitol-soy flour (MS) medium, especially actinorhodin (ACT) and calcium-dependent antibiotic (CDA), and disruption of *ohkAsav* in *S. avermitilis* also led to the similar phenotypes of impaired morphological differentiation and significantly increased oligomycin A production. DNA microarray analysis combined with real-time reverse transcription-PCR (RT-PCR) and RNA dot blot assay in the *S. coelicolor ohkA* deletion mutant confirmed the physiological results by showing the upregulation of genes involved in the biosynthesis of ACT, CDA, undecylprodigiosin (RED), a yellow type I polyketide (CPK, *SCO6273-6289*), and a sesquiterpene antibiotic, albaflavenone (*SCO5222-5223*). The results also suggested that the increased production of ACT and RED in the mutant could be partly ascribed to the enhanced precursor malonyl coenzyme A (malonyl-CoA) supply through increased transcription of genes encoding acetyl-CoA carboxylase (ACCase). Interestingly, DNA microarray analysis also showed that deletion of *ohkA* greatly downregulated the transcription of *chpABCDEFGH* genes essential for aerial mycelium formation by *S. coelicolor* on MS medium but significantly increased transcription of *ramS/C/R*, which is responsible for SapB formation and regulation and is normally absent on MS medium. Moreover, many other genes involved in development, such as *bldM/N*, *whiG/H/I*, *ssgA/B/E/G/R*, and *whiE*, were also significantly downregulated upon *ohkA* deletion. The results clearly demonstrated that OhkA is an important global regulator for both morphological differentiation and secondary metabolism in *S. coelicolor* and *S. avermitilis*.

Streptomyces species are Gram-positive, soil-dwelling, and filamentous bacteria. They are well known for producing a wide variety of important natural antibiotics and bioactive compounds currently used in medicine and agriculture. In response to nutrient deprivation, the *Streptomyces* colonies begin producing many secondary metabolites (e.g., antibiotics) at the onset of aerial mycelium formation. *Streptomyces coelicolor*, as the model species, has been used in the studies of morphological differentiation and antibiotic regulation in the genus *Streptomyces* for many years (20). It can generate at least four antibiotics, including blue-pigmented polyketide actinorhodin (ACT), red-pigmented prodigiosins (RED), calcium-dependent antibiotic (CDA), and an SCP1 plasmid-encoded antibiotic, methylenomycin (Mmy) (30). The regulation of antibiotic biosynthesis and morphological differentiation in *S. coelicolor* has been found to involve many different regulatory proteins, such as *bld*- and *whi*-encoded regulatory proteins and eukaryotic serine/threonine protein kinase, etc. (5, 9).

The two-component system (TCS), which is the predominant signal transduction system widely distributed in bacteria (46), has also been involved in the regulation of antibiotic biosynthesis and morphological differentiation in *S. coelicolor* (22). Bioinformatic analysis of the *S. coelicolor* genome reveals the presence of at least 67 paired TCSs (4, 22), many of which have been identified as being involved in either the production of secondary metabolites (e.g., *phoP-phoR*, *cutS-cutR*, *ecrA1-ecrA2*, and *rapA1-rapA2*) (8, 22, 33, 34, 45), development (*ragK-ragR*) (43), or both antibiotic biosynthesis and morphological differentiation (e.g., *afsQ1-afsQ2* and *absA1-absA2*) (3, 6, 23, 40, 44). In addition, there also exist 13 orphan response regulators (RRs) and 17 orphan histidine kinases (HKs) in *S. coelicolor* (22). Several of these orphan RRs have been characterized, and their roles in development and antibiotic production have been established (19, 49); however, no orphan HK has been studied so far.

In order to functionally identify the orphan HKs in *S. coelicolor*, we have constructed several deletion mutants of the orphan HK-encoding genes. After phenotype screening, we identified an orphan histidine kinase (designated OhkA, encoded by gene *SCO1596*) that plays global regulatory roles in both morphological differentiation and antibiotic biosynthesis

* Corresponding author. Mailing address: Key Laboratory of Synthetic Biology, Institute of Plant Physiology and Ecology, Shanghai Institutes for Biological Sciences, Chinese Academy of Sciences, Shanghai 200032, People's Republic of China. Phone: 86-21-54924172. Fax: 86-21-54924015. E-mail: whjiang@sibs.ac.cn.

† Supplemental material for this article may be found at http://jb.asm.org/.

▽ Published ahead of print on 22 April 2011.

TABLE 1. Strains and plasmids used in this study

Strain or plasmid	Description	Source or reference
E. coli strains		
DH5α	F$^-$ ϕ80d*lacZ*ΔM15 Δ*(lacZYA-argF)U169 deoR recA1 endA1 hsdR17*(r_K^- m_K^+) *supE44* λ$^-$ *thi-1 gyrA96 relA1*	Gibco-BRL
BW25113	K-12 derivative; Δ*araBAD* Δ*rhaBAD*	13
BW25113/pIJ790	BW25113 containing temperature-sensitive plasmid pIJ790, which encodes the λ RED recombination system	18
ET12567	*dam-13*::Tn*9 dcm-6 hsdM*	35
ET12567/pUZ8002	ET12567 containing the nontransmissible RP4 derivative plasmid pUZ8002	18
S. coelicolor strains		
M145	Wild type; SCP1$^-$ SCP2$^-$ *pgl*$^+$	29
M145Δ*ohkA*	M145 *ohkA*::*acc(3)IV*	This work
M145/pSET152AT	M145 with the control vector pSET152AT	This work
M145Δ*ohkA*/pSET152AT	M145Δ*ohkA* with pSET152AT	This work
M145Δ*ohkA*/pSETohkA	M145Δ*ohkA* with the complementation vector pSETohkA	This work
M145Δ*ohkA*/pSETohkAH159L	M145Δ*ohkA* with the mutated complementation vector pSETohkAH159L	This work
S. avermitilis strains		
NRRL 8165	Wild type; the model avermectin-producing strain	NRRL
8165Δ*ohkAsav*	NRRL 8165 *ohkAsav*::*acc(3)IV*	This work
8165/pIB141	NRRL 8165 with the control vector pIB141	This work
8165Δ*ohkAsav*/pIB141	8165Δ*ohkAsav* with the control vector pIB141	This work
8165Δ*ohkAsav*/pIBohkAsav	8165Δ*ohkAsav* with the complementation vector pIBohkAsav	This work
8165/pSET152AT	NRRL 8165 with the control vector pSET152AT	This work
8165Δ*ohkAsav*/pSET152AT	8165Δ*ohkAsav* with the control vector pSET152AT	This work
8165Δ*ohkAsav*/pSETohkA	8165Δ*ohkAsav* with the complementation vector pSETohkA	This work
Plasmids		
pIJ773	Plasmid containing the apramycin resistance gene *aac(3)IV* and *oriT* of plasmid RP4, flanked by FRT sites	18
pSET152	*oriT* RK2 plasmid carrying the apramycin resistance gene *aac(3)IV*	29
pSET152AT	pSET152 with insertion of the thiostrepton resistance gene (*tsr*) in the SphI site	This work
pIB139	Derived from pSET152, with the constitutive promoter *ermE**p	52
pIB141	pIB139 modified by inserting the thiostrepton resistance gene (*tsr*) downstream of *aac(3)IV*	This work
pIBohkAsav	pIB141 with the *ohkAsav* ORF cloned between NdeI and XbaI sites, in which *ohkAsav* was under the control of the constitutive promoter *ermE**p	This work
pSETohkA	pSET15AT with 2,120-bp DNA fragment containing the *ohkA* ORF, partial *SCO1597* ORF, and the possible promoter region of *SCO1597*	This work
pSETohkAH159L	*ohkA* ORF cloned in pSET152AT was mutated, resulting in pSETohkAH159L, in which histidine at position 159 in *ohkA* ORF encoding protein OhkA was changed to leucine	This work

in *S. coelicolor*. Deletion of *ohkA* in *S. coelicolor* led to drastically enhanced antibiotic biosynthesis, especially of ACT and CDA, and to impaired aerial hypha formation and sporulation on mannitol-soy flour (MS) medium. Disruption of an *ohkA* ortholog, *ohkAsav*, in *Streptomyces avermitilis* NRRL 8165 led to similar effects as those of *ohkA* deletion in *S. coelicolor*, suggesting that this orphan HK may represent a highly conserved signal transduction component involved in the regulation of both antibiotic biosynthesis and morphological differentiation among *Streptomyces* bacteria. In addition, DNA microarray analysis combined with real-time reverse transcription-PCR (RT-PCR) and RNA dot blot assay was employed to explore the possible regulatory mechanisms of *ohkA* in *S. coelicolor.*

MATERIALS AND METHODS

Bacterial strains and growth conditions. Bacterial strains and plasmids used in this study are listed in Table 1. *S. coelicolor* M145 and *S. avermitilis* NRRL 8165 were cultivated at 30°C on mannitol-soy flour (MS) agar (29) for spore suspension preparation, conjugal transfer, and phenotype observation. For determination of oligomycin A and avermectin production, BioK seed medium and BioK fermentation medium were employed with some modifications (10). *Escherichia coli* was cultivated at 37°C in LB medium or on LB agar with 50 μg ml^{-1} apramycin, 50 μg ml^{-1} thiostrepton, 50 μg ml^{-1} kanamycin, or 100 μg ml^{-1} ampicillin when necessary. Genetic manipulation of *S. coelicolor*, *S. avermitilis*, and *E. coli* was carried out according to the methods described by Kieser et al. (29) and Sambrook et al. (42).

Construction of the *ohkA* and *ohkAsav* gene deletion mutants. Gene deletion mutants of *S. coelicolor* M145 and *S. avermitilis* NRRL 8165 were constructed using a PCR targeting system previously established by Gust et al. (18). The mutant cosmids with *ohkA* or *ohkAsav* gene deletion were generated by electrotransforming *E. coli* BW25113 containing pIJ790 (with the genes encoding the λ Red system) and the cosmid harboring *ohkA* or *ohkAsav* gene with the PCR-amplified disruption cassette. The two disruption cassettes were obtained by PCR using template pIJ773 and primer pairs ohkAF/R and ohkAsavF/R, respectively (Table 1; see also Table S1 in the supplemental material). Cosmids with the deletion of *ohkA* or *ohkAsav* were verified by both PCR using primer pairs JohkAF/R and JohkAsavF/R (see Table S1 in the supplemental material), respectively, and SacI enzyme restriction analyses. The resulting cosmid [Δ*ohkA*::*aac(3)IV* or Δ*ohkAsav*::*aac(3)IV*] was electrotransformed into the nonmethylating *E. coli* ET12567/pUZ8002 and then transferred into *S. coelicolor* M145 or *S. avermitilis* NRRL 8165 by conjugal transfer. Finally, apramycin-resistant and kanamycin-sensitive exconjugants were selected, and the *ohkA* or

ohkAsav knockout mutant (M145Δ*ohkA* or 8165Δ*ohkAsav*) was confirmed by colony PCR with primers JohkAF/R and JohkAsavF/R, respectively.

Genetic complementation. The pSET152AT integrative vector, which was generated by inserting the thiostrepton resistance gene (*tsr*) in the SphI site of pSET152, was used for the construction of complementation vector with the wild-type (WT) *ohkA* gene. A 695-bp BglII-EcoRI fragment (containing the 5′ region of 198 bp encoding 66 amino acids [aa] of SCO1597, a 301-bp fragment including partial *SCO1598*, and the intergenic region between *SCO1597* and *SCO1598*) was amplified with primers ohkAcomF1/R1 (see Table S1 in the supplemental material); a 1,425-bp EcoRI-BglII fragment (containing the 3′ region of 150 bp encoding 50 aa of SCO1597 and the whole *ohkA* gene) was amplified with primers ohkAcomF2/R2 (Table S1). No error in amplification was found by DNA sequencing. The two fragments were ligated together with pSET152AT, which was cut with BamHI and treated with alkaline phosphatase (calf intestinal alkaline phosphatase [CIAP]; Takara, Japan), respectively, resulting in the complementation vector pSETohkA.

For the construction of the complementation vector with the *ohkAsav* gene, pIB141 vector, modified by inserting the thiostrepton resistance gene (*tsr*) downstream of the apramycin resistance gene *aac(3)IV* of pIB139 (Table 1), was employed and expression of *ohkAsav* was under the control of the constitutive promoter *ermE**p. The *ohkAsav* open reading frame (ORF) was amplified with primer pair ohkAsavcomF/R (see Table S1 in the supplemental material) and then cloned into NdeI and XbaI sites of pIB141, generating the complementation vector pIBohkAsav.

The resulting plasmids pSETohkA and pIBohkAsav were introduced into the *ohkA* and *ohkAsav* mutants, respectively, by *E. coli-Streptomyces* conjugation, and transformants were selected by thiostrepton resistance. pSET152AT and pIB141 were used as negative controls.

Site-directed mutagenesis of the putative phosphorylation site in OhkA. The *ohkA* gene cloned in the complementation vector pSETohkA was mutated using the QuikChange site-directed mutagenesis kit (Stratagene, La Jolla, CA), in which the putative phosphorylation site (histidine residue at position 159) of OhkA was replaced by leucine (L). Two complementary oligonucleotides, H159LF/R (see Table S1 in the supplemental material; mutation site is underlined; CACGAG was changed to CTCGAG, which is the XhoI enzyme site), were used. The clones with the correct site mutated were confirmed by DNA sequencing and then introduced into the *ohkA* mutant by conjugal transfer.

Microscopy. Cultures for fluorescence microscopy and scanning electron microscopy (SEM) were obtained by inserting sterile coverslips at a 45° angle into MS agar which was inoculated with the spores of M145 or its derivatives. For fluorescence microscopic analysis, coverslips were removed after incubation at 30°C for 5 days and fixed with methanol followed by washing with phosphate-buffered saline (PBS; pH 7.4). The samples were then stained with 4′,6-diamidino-2-phenylindole (DAPI; 25 μg/ml) at room temperature for 30 min, washed with PBS buffer, and then observed using a laser scanning confocal microscope, Fluoview FV1000 (Olympus, Tokyo, Japan). For SEM analysis, the coverslips were taken after 4 days of incubation at 30°C and fixed with fresh 2% glutaraldehyde (pH 7.2) and 1% osmium tetroxide, followed by complete drying in HCP-2 (Hitachi, Japan); coated with gold with a Fine Coater JFC-1600 (JEOL, Tokyo, Japan); and then examined with scanning electron microscopy (JSM-6360LV; JEOL, Tokyo, Japan).

Determination of antibiotic production. Actinorhodin (ACT) and undecylprodigiosin (RED) were determined as described before with some modifications (1, 34). Cultures of *S. coelicolor* wild-type M145 and its derivatives incubated on MS agar covered with plastic cellophane were collected at five time points (36, 48, 60, 72, and 94 h). For ACT measurement, KOH was added to the samples at a final concentration of 1 M; after 1 h at room temperature, the cultures were centrifuged at 8,000 × *g* for 10 min and absorbance of the supernatant was measured at the wavelength of 640 nm. For RED, the bacterial samples were first extracted with KOH to solubilize ACT as above, followed by centrifugation at 12,000 × *g* for 10 min, and the mycelial pellet was collected and washed with 0.9% NaCl twice. The resulting pellet was extracted with methanol (pH adjusted to 2.0 with HCl) overnight at room temperature, followed by centrifugation at 8,000 × *g* for 5 min, and absorbance of the supernatant was measured at the wavelength of 530 nm. The amount of ACT and RED was indicated as optical density at 640 nm (OD_{640})/g and OD_{530}/g (wet weight), respectively.

Assay of CDA was carried out according to the method described by Kieser et al. (29). Briefly, M145 and its derivatives were grown on MS agar for 48 h and then overlaid with *Staphylococcus aureus*-seeded soft LB agar (0.5% agar) with or without $Ca(NO_3)_2$ (a final concentration of 12 mM). After incubation overnight, a zone of inhibition, which is absent when $Ca(NO_3)_2$ is omitted, is diagnostic for CDA production.

Production of oligomycin and avermectin in *S. avermitilis* was determined by high-pressure liquid chromatography (HPLC) as described previously (11). Briefly, spores of different *S. avermitilis* strains (with the same OD_{450}) were inoculated into 30 ml BioK fermentation seed medium in 250-ml baffled flasks. After incubation for 40 h at 30°C on a rotary shaker at a speed of 200 rpm, cultures were transinoculated into three parallel 250-ml baffled flasks with 30 ml BioK fermentation medium by 5% inoculation and grown at 30°C, 200 rpm. Samples were taken at two time points, 5 and 10 days. For avermectin and oligomycin extraction, 7 ml methanol was added to 3 ml fermentation broth in a 20-ml tube and treated in an ultrasonic cleaner for 20 min. After centrifugation at 8,000 × *g* for 10 min, the supernatants were analyzed using an Agilent Eclipse XDB-C8 column (4.6 by 150 mm) maintained at 30°C, with a solvent system of methanol-water (85:15, vol/vol) and a flow rate of 0.9 ml/min. Commercial oligomycin A (98%, wt/wt) and avermectin B1a (95.9%, wt/wt) (Hisun Pharmaceutical Co. Ltd., Zhejiang, China) were used to make standard curves for quantitative determination.

RNA isolation and DNA microarray analysis. RNA samples used for DNA microarray analysis were prepared as previously described (34). Briefly, cultures of *S. coelicolor* wild-type M145 and the *ohkA* mutant incubated on MS solid medium with plastic cellophane were collected at three time points (48, 64, and 88 h), frozen immediately in liquid nitrogen, and then ground into powder. RNA isolation was performed with Trizol (Invitrogen, Carlsbad, CA) according to the procedures recommended by the manufacturer. Subsequently, RNA samples were digested with DNase I (Takara) followed by purification with the RNeasy minikit (Qiagen, Valencia, CA) to remove the contamination of chromosomal DNA. The quality and integrity of the RNA samples were checked by 1% agarose gel electrophoresis and spectrophotometry.

For DNA microarray experiments, Agilent GeneChip *S. coelicolor* M145 DNA arrays (custom-specific design) were used. Each gene was represented by one specific 60-nucleotide (60-nt) oligonucleotide probe with two replicates. Microarray assays, including labeling, hybridization, and washing, and microarray data normalization were performed by Shanghai Biochip Co. Ltd. (Shanghai, China) according to standard protocols provided by Agilent Technologies. Briefly, RNA samples were reverse transcribed to cDNA using Moloney murine leukemia virus (MMLV) reverse transcriptase (Invitrogen), followed by transcription with T7 RNA polymerase (New England BioLabs, Beverly, MA), resulting in aminoacyl-UTP (aaUTP; Ambion, Austin, TX)-labeled cRNA. After cRNA purification with an RNeasy minikit (Qiagen), cRNA was further labeled with Cy3 (for M145) and Cy5 (for the *ohkA* mutant), respectively. Hybridization was carried out at 65°C for 17 h with a constant rotation rate of 10 rpm. Arrays were scanned with 3-μm resolution using an Agilent DNA Microarray scanner (Agilent Technologies, Palo Alto, CA). Microarray data were normalized in the Agilent Feature Extraction software (Agilent Technologies) using total array signals and LOWESS algorithm options. The gene expression ratio (*n*-fold change; *ohkA* strain versus M145) was calculated from the normalized signal intensities.

qRT-PCR. The quantitative real-time RT-PCR (qRT-PCR) was performed to validate selected microarray data. The SYBR Premix ExTaq (Toyobo, Japan) kit was used according to the instructions provided by the manufacturer. The primers used in qRT-PCR are listed in Table S1 in the supplemental material. The reactions were carried out in a Rotor-Gene RG-3000 thermal cycler (Corbett Research, Australia), using the following conditions: 95°C for 2 min, followed by 40 cycles of 95°C for 15 s, 65°C for 20 s, and 72°C for 20 s. Three PCRs were performed in parallel for each transcript. The *hrdB* gene was used as an internal control. The level of RNA transcript in different samples was measured according to the number of cycles (C_T [threshold cycle]) needed for the reactions to reach a fixed threshold (T). The relative fold change of RNA transcript (mutant/WT) was determined using the $2^{-\Delta\Delta CT}$ method, in which $\Delta\Delta C_T = (CT_{\text{tested gene}} - CT_{hrdB})_{\text{mutant}} - (CT_{\text{tested gene}} - CT_{hrdB})_{\text{WT}}$. qRT-PCR was repeated three times with the same RNA samples.

RNA dot blot assay. RNA dot blot assay was performed in accordance with the method described by Amon et al. (2). In RNA dot blot assay, antisense RNA probes were used. For the generation of these probes, internal DNA fragments with a size between 0.3 and 0.5 kb of the tested genes were amplified by PCR (primers are listed in Table S1 in the supplemental material). The reverse primers contained the promoter region for T7 RNA polymerase, which allowed *in vitro* transcription of probes using RNA digoxigenin (DIG) labeling mix (Roche, Mannheim, Germany) and T7 RNA polymerase (New England BioLabs). RNA samples (1 μg per time point) were spotted onto positively charged nylon membranes (Hy-Bond; Amersham, GE Healthcare, United Kingdom) using a Bio-Dot microfiltration apparatus (Bio-Rad Laboratories, Hercules, CA). Hybridization of DIG-labeled RNA probes was detected with X-ray films (Kodak, Rochester, NY) using alkaline phosphatase-conjugated anti-DIG Fab fragments and the chemiluminescent substrate disodium 3-(4-methoxyspiro {1,2-

dioxetane-3,2′-(5′-chloro)tricyclo[3.3.1.1^{3,7}]decan}-4-yl)phenyl phosphate (CSPD) according to the manuals provided by the manufacturer (Roche). All experiments were carried out at least twice with RNA samples extracted from independent cultures. The *hrdB* gene, which encodes the principal sigma factor of *S. coelicolor* and is constantly transcribed throughout the time course, was used as a positive internal control.

Microarray data set accession number. The raw DNA microarray data set analyzed in the present paper has been submitted to the NCBI Gene Expression Omnibus under the accession number GSE26426.

RESULTS AND DISCUSSION

Genomic organization of *ohkA* gene and its homologs in streptomycetes. OhkA showed significant sequence identity to typical HKs (e.g., 35.4% identity in 257 amino acids overlapping with HydH in *E. coli*) (http://streptomyces.org.uk/). Bioinformatics analysis (http://smart.embl-heidelberg.de/) revealed that the domain architecture of OhkA was the same as the paradigmatic soluble, cytoplasmic-sensing HK NtrB, which was required for the assimilation of ammonia and the utilization of alternative N compounds in *E. coli* (36), indicating that OhkA might also be a soluble HK, in contrast with most of the membrane-bound HKs (36, 57). In addition to two typical domains, DHp (*d*imerization and *h*istidine *p*hosphotransfer domain) and CA (*c*atalytic and *A*TP-binding domain), OhkA and NtrB both contain a PAS domain at the N terminus (see Fig. S1A in the supplemental material), which is an important signaling module, implicated in monitoring light, oxygen, and small ligands as well as protein-protein interactions for homodimer or heterodimer formation (36, 48). However, no gene encoding a putative RR is located close to *ohkA*, so it appears to be an orphan HK.

BLAST analysis showed that OhkA homologs with high amino acid identity (approximately 70 to 99%) are widely distributed in streptomycetes (see Fig. S1B in the supplemental material) and some other complex actinomycetes, such as *Frankia* and *Thermobispora*. The genetic organization of the *ohkA* gene is displayed in Fig. S1C. Upstream of *ohkA* is the *SCO1597* gene, encoding a putative rRNA methylase. Although these two genes do not overlap, their shared intergenic region is very short (50 bp), suggestive of a possible operon (this was confirmed by RT-PCR analysis; data not shown). Immediately downstream of *ohkA* are *pheS* (*SCO1595*) and *pheT* (*SCO1594*), which encode alpha and beta chains of a putative phenylalanyl-tRNA synthetase, respectively. Interestingly, this genetic organization is highly conserved among closely related streptomycetes (Fig. S1C). The conserved domain structure, sequence similarity, and conserved genetic organization of *ohkA* and its homologs suggest that they may have similar physiological roles.

OhkA regulates both morphogenesis and antibiotic biosynthesis in *S. coelicolor*. The mutant M145Δ*ohkA* with the entire *ohkA* gene deleted in *S. coelicolor* was generated using a PCR targeting system (18). A growth experiment showed that the *ohkA* mutant (M145Δ*ohkA*/pSET152AT) and M145 (M145/pSET152AT) had quite different growth rates. At the early stage (before 48 h), the mutant grew slower than M145; as time continued, from 60 h to 84 h it continued to grow and achieved a higher biomass, while M145 and the complemented strain (M145Δ*ohkA*/pSETohkA) ceased growth (Fig. 1A). Meanwhile, aerial mycelium and spore formation were also quite different. M145 formed abundant white aerial mycelium at 36 h, followed by gray-color formation from 48 h. However, for the *ohkA* mutant, aerial mycelium appeared much later, as shown in Fig. 1B; at 48 h very sparse aerial hyphae were formed. Until 60 h, the *ohkA* mutant was covered with only a thin layer of aerial mycelium, and interestingly, from 72 h onward the colony surface began to show the pink color. In addition, compared with the wild-type strain M145, which normally produces very little or no pigmented antibiotic on MS agar, the *ohkA* deletion mutant produces much ACT and CDA and a low level of RED (Fig. 1C).

When the *ohkA*-null mutant spores were inoculated on MS plates, a significant reduction in aerial mycelium formation and impaired sporulation were observed by scanning electron microscopy (SEM) after incubation for 4 days. As shown in Fig. 1D, in contrast to M145, which was covered with abundant straight or loosely coiled spore chains, the *ohkA* mutant might form two types of aerial hyphae: (i) nonsporulating, sparse, irregular long and straight ones and (ii) a minority (probably not so long) that were capable of developing into very short spore chains or single spores. In addition, a significant number of the mutant aerial hyphae are branched.

To further dissect the developmental differences between the *ohkA* mutant and the wild-type strain, they were stained with DAPI and visualized with confocal fluorescence microscopy. DNA staining clearly visualizes the completed segregation and condensed chromosomes in the wild-type strain. In contrast, the mutant strain formed very short spore chains and showed rather irregular chromosomal segregation and condensation. DNA staining was uneven in the mutant, with only a few spores very strongly stained and the majority of them weakly stained. Fluorescence microscopy also revealed, compared with M145, that chromosomal DNA in the spores of the mutant was distributed at irregular intervals (Fig. 1E).

To confirm that the mutant phenotype resulted from the absence of *ohkA* rather than random mutations elsewhere in the genome, the wild-type *ohkA* gene with its putative promoter present on the integrative vector pSET152AT was introduced into the mutant. The phenotype of the mutant could be restored to that of M145. After incubation on MS plates at 30°C for 4 days, in contrast to the mutant, both the wild type and the complemented strain were covered with abundant straight or loosely coiled spore chains which often contained several tens of spores (Fig. 1D) as observed by SEM, and antibiotic biosynthesis was restored to the wild-type levels (Fig. 1C). These results conclusively demonstrated that OhkA is involved in the regulation of both antibiotic biosynthesis and morphological differentiation in *S. coelicolor*.

The putative phosphorylation site (H159) is necessary for OhkA function. Bioinformatics analysis showed that His at position 159 might be the phosphorylation site of OhkA (see Fig. S1B in the supplemental material). To verify this possibility, we studied the effect of inactivating the OhkA phosphorylation site on antibiotic production and morphological differentiation. The putative phosphorylation site (H159) of OhkA was mutated to leucine (L) by site-directed mutagenesis using the QuikChange site-directed mutagenesis kit, and the correct mutant cloned in pSET152AT [pSETohkA(H159L)] was transferred into M145Δ*ohkA* by conjugation as described in Materials and Methods. The empty vector pSET152AT and

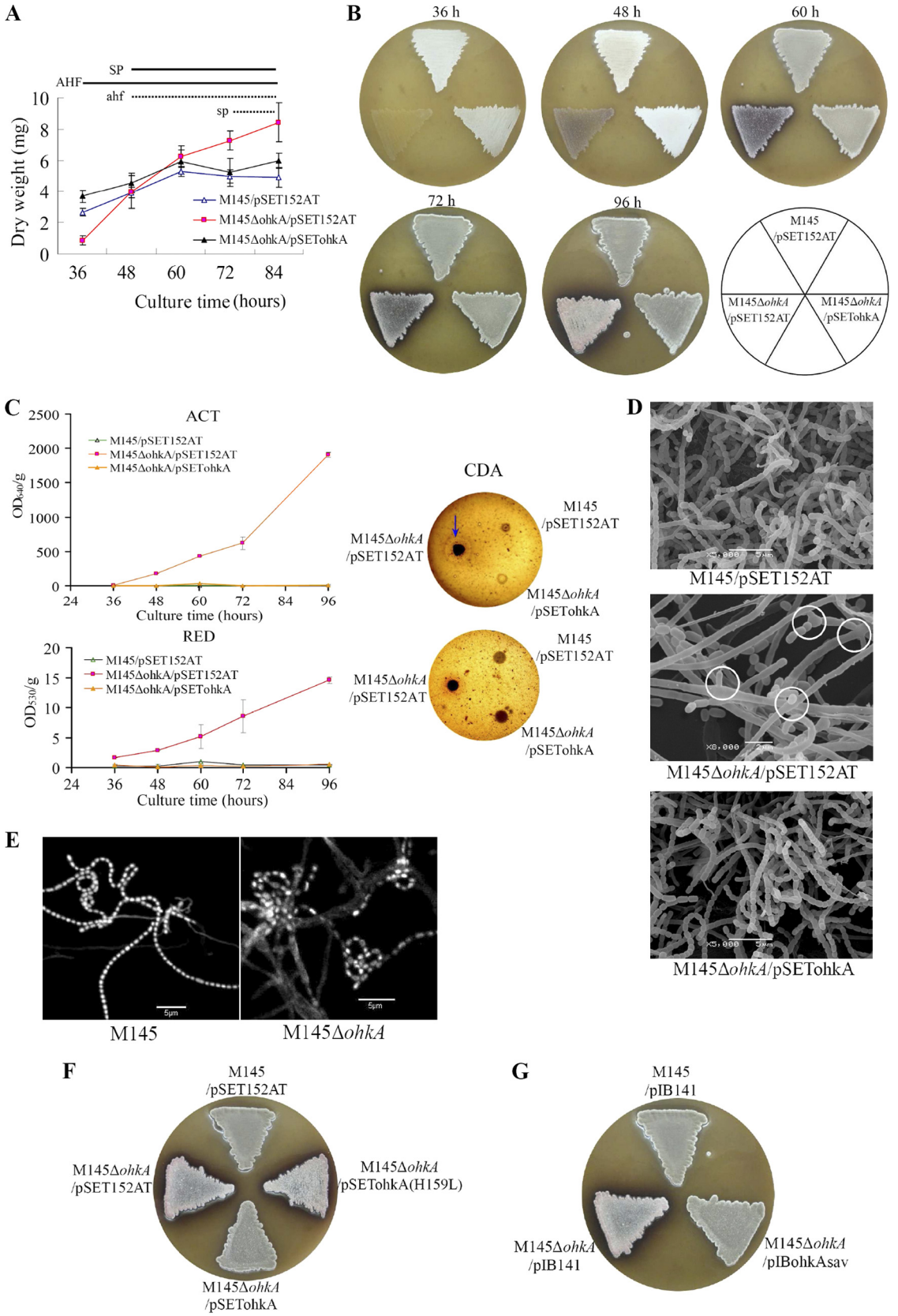

FIG. 1. Phenotypes of the *ohkA* deletion mutant compared with the wild-type strain M145. (A) Pregerminated spore suspensions from *S. coelicolor* M145/pSET152AT (△), the *ohkA* mutant (M145Δ*ohkA*/pSET152AT; ■), and the complemented strain (M145Δ*ohkA*/pSETohkA; ▲) were cultured on MS agar with cellophane discs at 30°C. Cultures were taken and dried at the time points indicated. Experiments were done in

pSETohkA were used as negative and positive controls, respectively. We found that, the mutant M145Δ*ohkA* with introduction of pSETohkA(H159L) showed pink colony and antibiotic overproduction, the same phenotype as the mutant strain with empty vector (Fig. 1F), indicating that this histidine residue is functionally significant and required for the role of OhkA *in vivo*.

OhkAsav (*SAV_6741*) from *S. avermitilis*, a homolog of OhkA, has similar functions. As described above, OhkA homologs from different streptomycetes had high sequence similarity and conserved genetic organization (see Fig. S1 in the supplemental material), prompting us to suggest that these homologs may have similar functions as OhkA does in *S. coelicolor*. To test this hypothesis, the *ohkA*-homologous gene *ohkAsav* from *S. avermitilis* was cloned into pIB141 vector under the control of *ermE**p and transferred into the *ohkA* mutant. The results showed that introduction of the *ohkAsav* gene into the *ohkA* mutant could readily restore the phenotype changes of the *S. coelicolor ohkA* mutant (Fig. 1G), indicating that *ohkAsav* may function similarly to *ohkA*.

To further identify the function of *ohkAsav*, we constructed the *ohkAsav* deletion mutant in *S. avermitilis* and found that deletion of the *ohkAsav* gene also had global effects on both antibiotic biosynthesis (e.g., significantly increased oligomycin A production) and development (e.g., formation of thin aerial mycelium and impaired sporulation) (Fig. 2A to C) in *S. avermitilis*. The effects could be rescued by complementation with the wild-type *ohkAsav* or the *ohkA* gene from *S. coelicolor* (as shown in Fig. 2A and B). However, no notable difference in avermectin biosynthesis was found between the *ohkAsav* deletion mutant and the wild-type strain (data not shown).

Comparison of transcription profiles of the *ohkA* mutant and its wild-type strain M145. To explore the possible regulatory mechanisms of OhkA on both antibiotic production and morphological differentiation, we compared the global transcription profiles between the *ohkA* deletion mutant and its parental strain M145 using DNA microarrays. Strains were grown on MS agar with plastic cellophane, and cultures were harvested for RNA preparation at three time points, 48, 64, and 88 h. Pairwise comparison showed that, across three time points, there are a total of 1,078 genes upregulated and 1,277 downregulated at least 2-fold (ratio: mutant/wild type, $\geq$2.0 or $\leq$0.5) in the mutant compared with M145. However, it should be noted that only one sample was microarray analyzed for each time point (with two technical replicates); the significance of the gene expression changes needs to be further verified. To do so, we verified the DNA microarray data by qRT-PCR for 14 selected genes as shown in Table 2. In general, good consistency was found between DNA microarray and RT-PCR data in terms of the trends of the changes. Additionally, good consistency between the phenotype changes arising from *ohkA* deletion and the changes of the genes involved in these phenotypes also supported the overall quality of microarray analysis. Key functional genes whose transcription was down- or upregulated over 2-fold due to the deletion of the *ohkA* gene and further confirmed by qRT-PCR and RNA dot blot assay are described below (see Table S2 in the supplemental material).

Effects of *ohkA* deletion on the transcription of secondary metabolism. In agreement with the much higher production of ACT and CDA and slightly enhanced RED production in the *ohkA* mutant compared with M145, transcription profiles showed that, the majority of ACT and CDA biosynthetic gene clusters were upregulated more than 2-fold at the tested time points, while transcription of RED genes was mainly confined to the earliest time point (48 h), as shown in Fig. 3A. In addition, we found that the transcriptional levels of two other antibiotic biosynthetic gene clusters, a type I polyketide synthase gene cluster (*SCO6273-6288*) responsible for the biosynthesis of a novel yellow-pigmented secondary metabolite (CPK) with antibacterial activity (17, 39) and a gene cluster (*SCO5222-5223*) for biosynthesis of the sesquiterpene antibiotic albaflavenone (58), were enhanced as well (Fig. 3A).

DNA microarray analysis also showed that the transcriptional levels of the pathway-specific regulators of four secondary metabolites (*actII-ORF4* for ACT, *redD* for RED, *cdaR* for CDA, and *cpkO* for CPK) were all increased significantly in the *ohkA*-null mutant compared to M145, which was confirmed by qRT-PCR analysis (Table 2) and RNA dot blot assay (Fig. 3C). As shown from the RNA dot blot assay, transcription of *actII-*

triplicate. AHF and SP indicate phases of aerial hypha formation and sporulation, respectively, of M145/pSET152AT and the complemented strain, while ahf and sp indicate the corresponding phases of the *ohkA* mutant (M145Δ*ohkA*/pSET152AT). Growth was calculated as mg (dry weight). (B) Phenotypes of M145/pSET152AT, M145Δ*ohkA*/pSET152AT, and the complemented strain M145Δ*ohkA*/pSETohkA on MS agar. The plates were incubated at 30°C for the indicated time points. The surface of the mutant strain M145Δ*ohkA*/pSET152AT displayed pink color from 72 h onward. (C) Determination of antibiotic production in M145Δ*ohkA*/pSET152AT, relative to M145/pSET152AT and the complemented strain M145Δ*ohkA*/pSETohkA. For ACT and RED measurement, cultures were grown on MS agar at 30°C and taken at the indicated time course; ACT and RED production was calculated as OD_{640}/g and OD_{530}/g (wet weight), respectively. Experiments were performed in triplicate. For CDA, 1-μl spore suspensions with the same OD_{450} were grown on MS agar at 30°C for 48 h and then overlaid with *Staphylococcus aureus*-seeded soft LB agar with (upper panel) or without (lower panel) $Ca(NO_3)_2$. A zone of inhibition (indicative of CDA activity) was detected in the presence of $Ca(NO_3)_2$, which is indicated by the blue arrow. (D) Scanning electron micrographs (SEM) showing the developmental changes of the *S. coelicolor ohkA* mutant (with pSET152AT) compared with M145 (with pSET152AT) and the complemented strain M145Δ*ohkA*/pSETohkA. Cultures were grown on MS medium for 4 days at 30°C. Branched aerial hyphae are shown by white circles. Scale bars are shown in the panels. (E) DNA content of *S. coelicolor* M145 and the *ohkA* mutant revealed by DAPI staining. The *ohkA* mutant is disturbed by DNA condensation and segregation. DNA staining was uneven in the *ohkA* mutant, with only a few spores very strongly stained (indicated by white arrows) and the majority of them weakly stained. Cultures were grown on MS agar for 4 days at 30°C. (F) Spore suspensions of M145/pIB141, M145Δ*ohkA*/pIB141, the complemented strain M145Δ*ohkA*/pSETohkA, and the mutant strain with plasmid-borne mutated *ohkA* (H159L) (M145Δ*ohkA*/pSETohkAH159L) were plated on MS medium and incubated at 30°C for 4 days. The surface of the mutant strains M145Δ*ohkA*/pSET152AT and M145Δ*ohkA*/pSETohkAH159L showed pink color. (G) Spore suspensions of M145/pIB141, M145Δ*ohkA*/pIB141, and the complemented strain M145Δ*ohkA*/pIBohkAsav were plated on MS medium and incubated at 30°C for 4 days. The impaired morphological differentiation of the *ohkA* mutant could be complemented by the introduction of the *ohkA*-homologous gene *ohkAsav* from S. *avermitilis*.

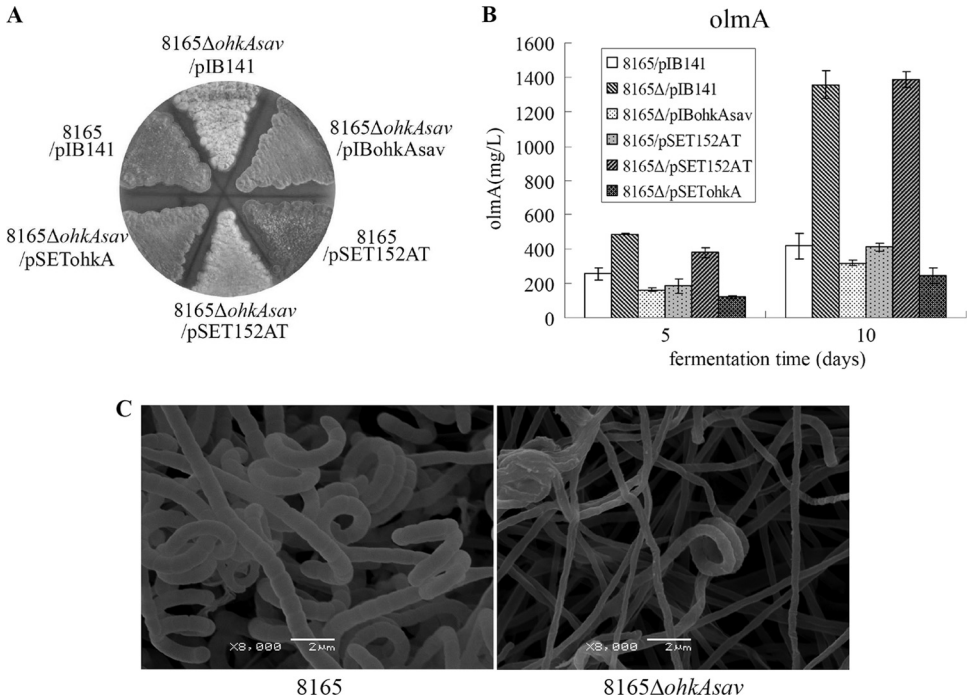

FIG. 2. Phenotypes of the *ohkAsav* mutant in contrast to the wild-type strain *S. avermitilis* NRRL 8165. (A) The defective sporulation of the *ohkAsav* mutant could be rescued by the complementation with the wild-type gene *ohkAsav* and *ohkA* from *S. coelicolor* when grown on MS medium. The white appearance of 8165Δ*ohkAsav* with pSET152AT or pIB141 was due to the failure to produce the gray-pigmented spores. These strains were cultured on MS medium for 10 days. (B) Overproduction of oligomycin A (olmA) assayed by HPLC in the *ohkAsav* mutant (8165Δ/pSET152AT or 8165Δ/pIB141) was restored by the complementation with *ohkAsav* gene (strain 8165Δ/pIBohkAsav) or *ohkA* gene from *S. coelicolor* (strain 8165Δ/pSETohkA). After incubation in fermentation broth for 5 and 10 days, cultures were extracted with methanol and analyzed by HPLC. Error bars indicate the standard deviations from three parallel flasks. (C) Scanning electron micrographs of the aerial hyphae and spores of NRRL 8165 (left panel) and the *ohkAsav* deletion mutant (right panel). The *ohkAsav* mutant showed abnormal development, including formation of thin aerial hyphae and impaired sporulation. Both strains were grown on MS medium for 10 days. Scale bars are shown in both panels.

ORF4 was almost invisible in M145 throughout the time points tested; however, upon *ohkA* deletion, its transcription was drastically elevated and showed the characteristics of growth phase dependence. The level of *hrdB* transcript was constant in all of the three strains throughout the time points, thus providing an effective positive control in the RNA dot blot assay. As a negative control, the *ohkA* transcript was nearly undetected in the *ohkA* mutant as expected. We also found that, in M145, a

TABLE 2. qRT-PCR analysis[a]

No.	Gene name	SCO no.	Function of gene product	Factor of transcription in real-time PCR (mean ±SD)		DNA microarray (mean)[b]	
				48 h	64 h	48 h	64 h
1	*kasO*	SCO6280	Regulatory protein	129.62 ± 25.51	6.85 ± 1.40	2.33	1.77
2	*actII-ORF4*	SCO5085	Actinorhodin cluster activator protein	2.23 ± 0.26	148.83 ± 70.12	5.65	13.65
3	*ramS*	SCO6682	Hypothetical protein	31.55 ± 8.06	725.77 ± 61.37	4.31	7.42
4	*cdaR*	SCO3217	Transcriptional regulator	12.70 ± 2.42	9.51 ± 1.00	2.31	2.22
5	*redD*	SCO5877	Transcriptional regulator	31.36 ± 6.49	15.33 ± 2.34	2.93	1.62
6	*scbA*	SCO6266	ScbA protein	13.07 ± 1.65	5.12 ± 1.58	2.21	3.74
7	*bldN*	SCO3323	RNA polymerase sigma factor	0.09 ± 0.01	0.06 ± 0.01	0.18	0.09
8	*wblA*	SCO3579	Regulatory protein	0.03 ± 0.01	0.07 ± 0.02	0.05	0.05
9	*chpB*	SCO7257	Secreted protein	0.05 ± 0.01	0.07 ± 0.01	0.05	0.07
10	*ssgA*	SCO3926	Regulator	0.06 ± 0.01	0.17 ± 0.02	0.29	0.27
11	*bldD*	SCO1489	DNA-binding protein	0.61 ± 0.05	0.46 ± 0.03	0.63	0.30
12	*whiG*	SCO5621	RNA polymerase sigma factor	0.32 ± 0.07	0.22 ± 0.05	0.19	0.22
13	*cvnD9*	SCO1627	ATP/GTP binding protein	0.27 ± 0.03	ND[c]	0.28	0.32
14	*cvnD11*	SCO0585	ATP/GTP binding protein	0.08 ± 0.06	ND	0.14	0.19

[a] RNA samples isolated from cultures of M145 and the *ohkA* mutant grown on MS agar covered with cellophane were used in qRT-PCR. The experiments were done in triplicate and repeated three times with RNA from independent cultures. The values reported are the means (± standard deviations) of three independent qRT-PCR analyses.

[b] Averages of two microarray signal ratios (mutant/wild type) from the specific 60-nt probe replicates for each gene.

[c] ND, not measured.

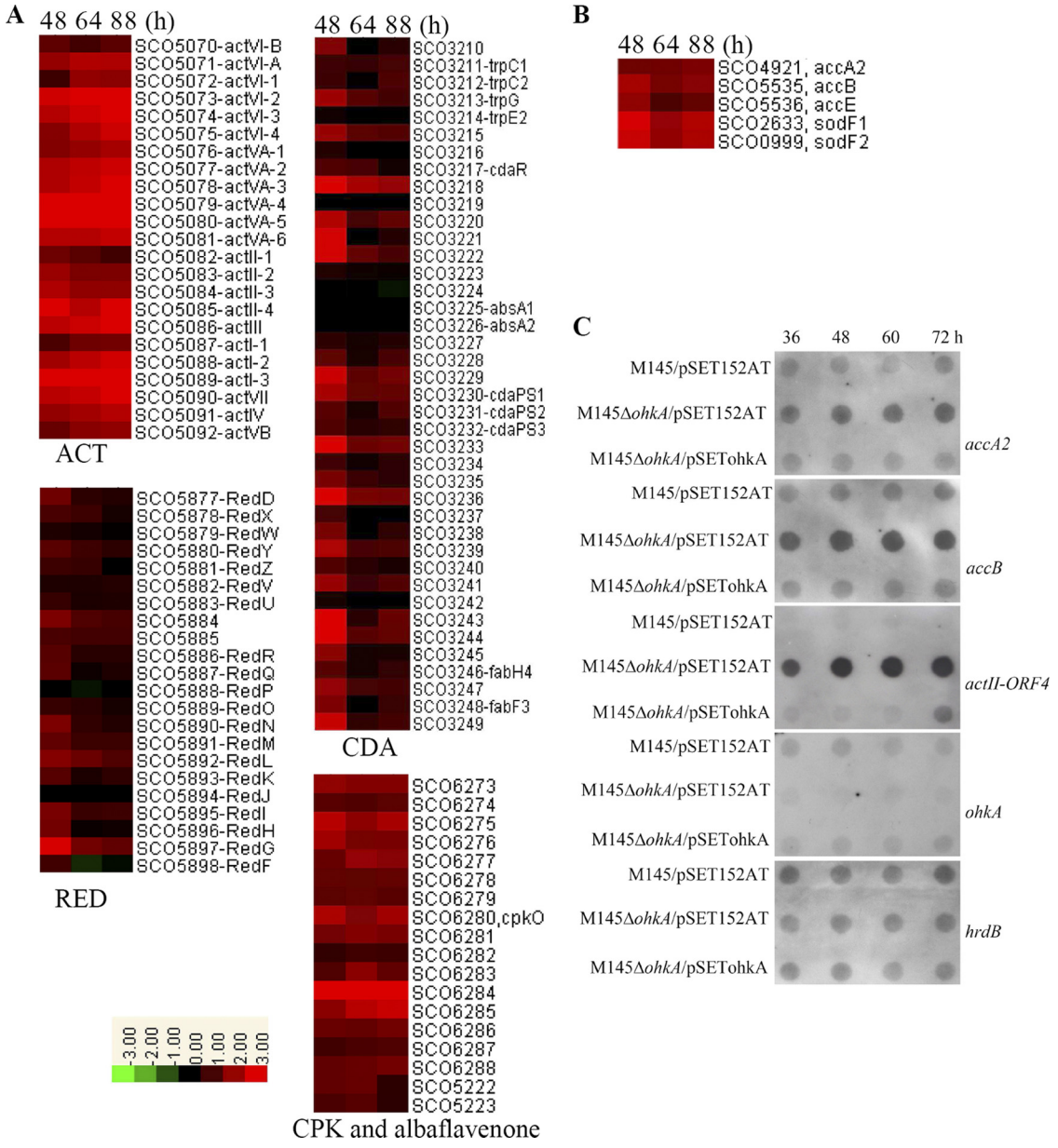

FIG. 3. Heat maps and RNA dot blot assays of selective gene clusters involved in antibiotic biosynthesis in *S. coelicolor*. (A and B) Transcription profiles of antibiotic biosynthetic gene clusters (ACT, RED, CDA, CPK, and albaflavenone) (A) and some primary metabolism genes in the *ohkA* mutant (B), compared with M145. RNA samples from M145 and the *ohkA* mutant were isolated at the indicated time points on MS medium. The relative changes of gene transcription are determined using $\log_2$(ratio of mutant/WT) and shown on a color scale, with red representing an increase in transcript abundance and green indicating a decrease in the *ohkA* mutant, relative to M145. Black represents unchanged expression levels. (C) RNA dot blot assay comparing the transcription of selected genes from panels A and B in M145/pSET152AT, M145Δ*ohkA*/pSET152AT, and M145Δ*ohkA*/pSETohkA. *hrdB* and *ohkA* were used as positive and negative controls, respectively. RNA samples were isolated at the indicated time points on MS medium, and 1 μg RNA per time point was spotted onto positive charged nylon membranes.

low constant mRNA level of the *ohkA* gene was detected throughout the time course, indicating that *ohkA* is transcribed constitutively. Transcriptional alterations of *actII-ORF4* and *ohkA* could be easily rescued by introduction of the *ohkA* gene (Fig. 3C). These data conclusively demonstrated that OhkA negatively regulated secondary metabolism by repressing directly or indirectly the pathway-specific activators in this microorganism.

Interestingly, there is no obvious transcriptional change of *redZ* encoding the orphan response regulator RedZ implicated in the positive control of *redD* transcription (19), suggesting that it might be one of the targets for OhkA. Since we have shown that there is no autophosphorylation activity of OhkA *in vitro*, other methods, such as yeast/bacterial two-hybrid assay, needed to be used to verify this possibility in the following study. We also showed that *ohkA* deletion had no effect on the transcription of TCS *absA1/A2*, which is clustered with CDA biosynthetic genes in the genome and can negatively regulate the biosynthesis of CDA, RED, and ACT (Fig. 3A).

DNA microarray analysis also revealed that the *scbA* gene involved in the synthesis of γ-butyrolactone signaling molecule SCB1 (47) was upregulated in the *ohkA* mutant, which was confirmed by qRT-PCR (Table 2). However, no obvious transcription change was found for the *scbR* gene, which encodes SCB1 binding protein. It was previously suggested that ScbR can repress the transcription of *cpkO* (pathway-specific regulator of CPK biosynthesis) through binding to its promoter region, resulting in lower CPK expression, and addition of SCB1 can eliminate the DNA binding and lead to high-level CPK production (47). It is thus speculative that upregulated transcription of *cpk* genes upon *ohkA* deletion might be the result of higher transcription of *scbA* that will elicit SCB1 accumulation and then relieve *cpkO* repression.

Effects of *ohkA* deletion on the transcription of primary metabolism genes. Precursors for the secondary metabolite biosynthesis are generally formed from primary metabolism through the Embden-Meyerhof pathway (EMP) (55). From DNA microarray analysis combined with RNA dot blot assay (Fig. 3B and C), we showed that deletion of *ohkA* significantly induced the expression of a gene complex including *accA2* (*SCO4921*), *accB* (*SCO5535*), and *accE* (*SCO5536*), which encodes the multienzyme complex acetyl coenzyme A (acetyl-CoA) carboxylase (ACCase) converting acetyl-CoA to malonyl-CoA in *S. coelicolor* (41). Malonyl-CoA and/or acetyl-CoA is the same precursor(s) for the biosynthesis of ACT and RED. Therefore, the increased expression of *accA2*/*B*/*E* should lead to higher malonyl-CoA formation and ACT and RED overproduction, which was in good agreement with a previous report on *S. coelicolor* (41), suggesting that OhkA plays a negative role in precursor supply for ACT and RED production in *S. coelicolor*.

We also found that two superoxide dismutase genes (*sodF1*/*sodF2*, SCO2633/SCO0999) which are involved in cellular resistance to toxic effects caused by oxidants were upregulated in the *ohkA* mutant (Fig. 3B). An earlier study demonstrated that transcription of *sodF1*/*F2* in *S. coelicolor* was enhanced upon overexpression of pathway-specific regulator ActII-ORF4 (21). Recently, it was also reported that overexpression of two superoxide dismutase genes, *sod1*/*sod2*, from *Streptomyces peucetius* can increase the clavulanic acid (CA) level in *Streptomyces clavuligerus* and RED production in *Streptomyces lividans* (25).

Effects of *ohkA* deletion on transcription of developmental genes. (i) Genes associated with aerial mycelium formation. In *S. coelicolor*, there are two classes of surface-active molecules, SapB and the chaplins, which are important for aerial hypha formation by reducing the surface tension at the air-colony interface (7). Early studies showed that the biosurfactant activities of both SapB and the chaplins are needed for normal aerial hypha formation on rich medium, such as R2YE. However, on mannitol-containing medium (such as MS), *S. coelicolor* normally does not produce SapB molecules and needs only chaplins for aerial morphogenesis (7). Comparison of the global transcription profiles of M145 and the *ohkA* deletion mutant grown on MS medium revealed that transcription of all eight chaplin genes, *chpA* to *chpH*, was downregulated in the *ohkA* mutant, whereas the *ram* genes (*ramC* and *ramS*) responsible for the production of SapB (7, 54) were significantly elevated at all time points tested, 48, 64, and 88 h (Fig. 4A; Table 2). Although no obvious changes in expression of *ramR* were observed in the microarray data, *ramR* transcription in the mutant was up 2-fold compared with that in M145 as measured by qRT-PCR analysis (Table 2). These observations were in good agreement with previous evidence that *ramC*/*S* was under the positive regulation of *ramR* (26, 37). To further confirm these changes, an RNA dot blot assay for *chpD* and *ramS*/*R* was carried out. The results showed that, compared with high-level transcription of the *chpD* gene in M145, transcription of this chaplin gene was negligible in the *ohkA* mutant. In contrast, while *ramS*/*R* transcription was almost invisible in the wild-type strain, their expression was significantly enhanced upon *ohkA* deletion (Fig. 4B). These results clearly indicated that OhkA plays a differential role in the regulation of these two surface-active molecules, positive for the chaplin proteins and negative for SapB production.

It has been suggested that the formation of chaplins is under strict regulation by the *bld* cascade (7, 14). In this study, several *bld* genes in the *ohkA* mutant, including *bldB*, *bldD*, *bldM*, and *bldN*, were found to be downregulated, especially *bldN*, whose transcription was nearly undetectable, as verified by RNA dot blot assay (Fig. 4A and B). Previous reports showed that, on rich medium R2YE, the eight chaplin genes (*chpA* to *chpH*) were indirectly under the control of sigma factor σ^N and also its downstream target gene *bldM*, encoding the atypical response regulator BldM. Deletion of *bldN* or *bldM* would result in the drastically decreased expression of the *chp* genes (14). Here, we showed that in the *ohkA*-null mutant, transcription of both *bldN* and *bldM* was significantly reduced. Furthermore, transcription of all the genes which have been identified as being under the control of *bldN* (14), including the eight *chp* genes, *SCO1088*, *SCO1089*, *SCO3714*, *SCO4002* (*nepA*), and *SCO5819* (*whiH*), etc., was found to be significantly decreased in the *ohkA* mutant, implying that the regulation of *ohkA* on the *chp* genes was possibly mediated by the functions of *bldN*, and *bldM* may also be included. The data described above strongly suggested that when *S. coelicolor* was grown on MS agar, chaplin genes were positively regulated by *bldN* as well.

In addition, *bldB* is required for *S. coelicolor* aerial hypha formation on any medium and chaplins were not detectable in the *bldB* mutant (7), suggesting that downregulation of *chp* genes in the *ohkA* mutant might be partly associated with the lower transcription of *bldB*.

(ii) Genes associated with spore formation and maturation. A number of regulatory genes have been identified as being necessary for initiating sporulation in *S. coelicolor*, such as *whi* and *ssg* genes. These genes could be divided into "early" and "late" sporulation genes depending on whether the relevant mutants undergo hyphal septum formation (9, 15). *whiA*/*B*/*G*/*H*/*I*/*J* and *ssgA*/*B*/*R* are considered early genes, which are required for the expression of late genes, including *sigF* and *whiD*. In the *ohkA* mutant, we found that mRNAs of one early *whi* gene, *whiG*, which encodes an early-sporulation-specific RNA polymerase sigma factor; two of its direct target genes, *whiH* and *whiI*; and one late sporulation gene, *whiD*, were significantly reduced at all three time points tested (Fig. 5A). In addition, transcription of *ssgA* and its regulatory gene *ssgR*, essential for sporulation-specific septum formation (50, 51, 53), was downregulated more than 2-fold. Moreover, several *ssgA*-like genes, *ssgB*, *ssgE*, and *ssgG*, involved in septum for-

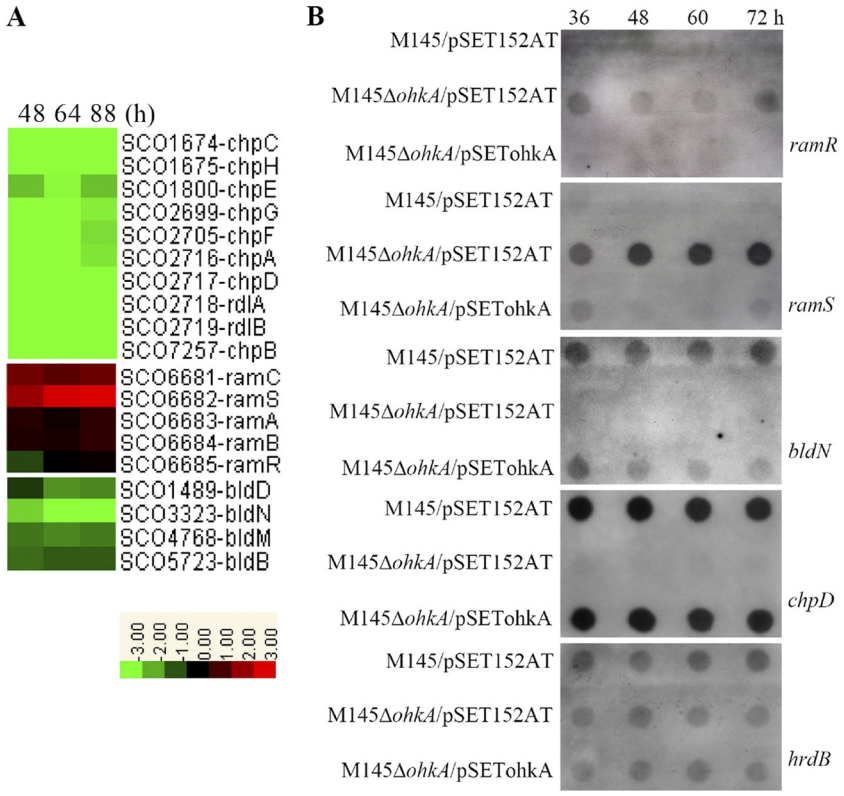

FIG. 4. Heat maps and RNA dot blot assays of selective gene clusters involved in morphological differentiation in *S. coelicolor*. (A) Transcription profiles of genes associated with aerial mycelium formation in the *ohkA* mutant, compared with M145. RNA samples from M145 and the *ohkA* mutant were isolated at the indicated time points on MS medium. The color representation is as described in the legend for Fig. 3. (B) RNA dot blot assay comparing the transcription of selected genes from panel A in M145/pSET152AT, M145Δ*ohkA*/pSET152AT, and M145Δ*ohkA*/pSETohkA. *hrdB* was used as a control for RNA loading levels.

mation, autolytic spore separation, and exact septum localization (38, 53), respectively, were significantly decreased as well (Fig. 5A).

Transcription of the *whiE* gene cluster (ORFs I to VIII) responsible for the synthesis of spore pigment (a type II polyketide compound) in *S. coelicolor*, including a likely operon of seven genes (ORFs I to VII) and one divergently transcribed gene (ORF VIII) (27, 56), was significantly decreased in the *ohkA* mutant compared with M145, as shown in Fig. 5A and B. Moreover, a late-sporulation-specific RNA polymerase sigma factor, σ^F, encoded by *sigF*, which directs the expression of *whiE-ORFVIII* (27), was greatly downregulated as well in the mutant (Fig. 5A). Surprisingly, in the wild-type strain M145, transcription of *sigF* was detected earlier, at 36 h, which is inconsistent with previous work showing that *sigF* was expressed exclusively during sporulation when cultured on minimal medium (MM) (28), prompting us to suggest that transcription profiles of *sigF* might be quite different when *S. coelicolor* is grown on different media. An earlier study reported that disruption of *whiE-ORFVIII* resulted in spore color change (from gray to greenish). In addition, ectopic expression of different combinations of *whiE* and ORFs would lead to different spore pigment-related metabolites in or on the mycelium (56). So, it is speculative that the pink color of the *ohkA* mutant might be the result of decreased transcription of these *whiE* genes. Another possibility is the ectopic production of ACT and RED in aerial mycelium of the *ohkA* mutant, especially ACT, which has been described in the recent study carried out by Fowler-Goldsworthy (16).

DNA microarray data also revealed that deletion of *ohkA* not only nearly abolished expression of the chaplin genes but also led to drastically reduced transcription of the two rodlin genes encoding the other components identified as the *S. coelicolor* hydrophobic sheath, the rodlins RdlA and RdlB (Fig. 4A). It was previously demonstrated that expression of *rdlA* and *rdlB* is almost absent in the Δ*chpABCDEFGH* strain (12). We thus speculated that downregulation of *rdlAB* transcripts might be the result of significantly reduced expression of chaplin family genes. A previous report found that deletion of one or both rodlin genes did not affect the formation of aerial hyphae and spores; however, the spores of the *rdl*-null mutant had a disordered surface ultrastructure of fine chaplin filaments. However, due to the low resolving capability of the EM available, we have not seen any phenotype changes of the *ohkA* mutant spore surface. From these results presented here, we could conclude that OhkA had a pleiotropic impact on the control of aerial hypha formation and the sporulation process in *S. coelicolor* through the effect on *bld*, *whi*, and *ssg* genes.

Effects of *ohkA* deletion on other regulators involved in antibiotic biosynthesis. In the *S. coelicolor* genome, there exist 13 conservons which typically consist of a cluster of four genes (*cvnA* to *cvnD*): *cvnA*, encoding a sensor histidine kinase ho-

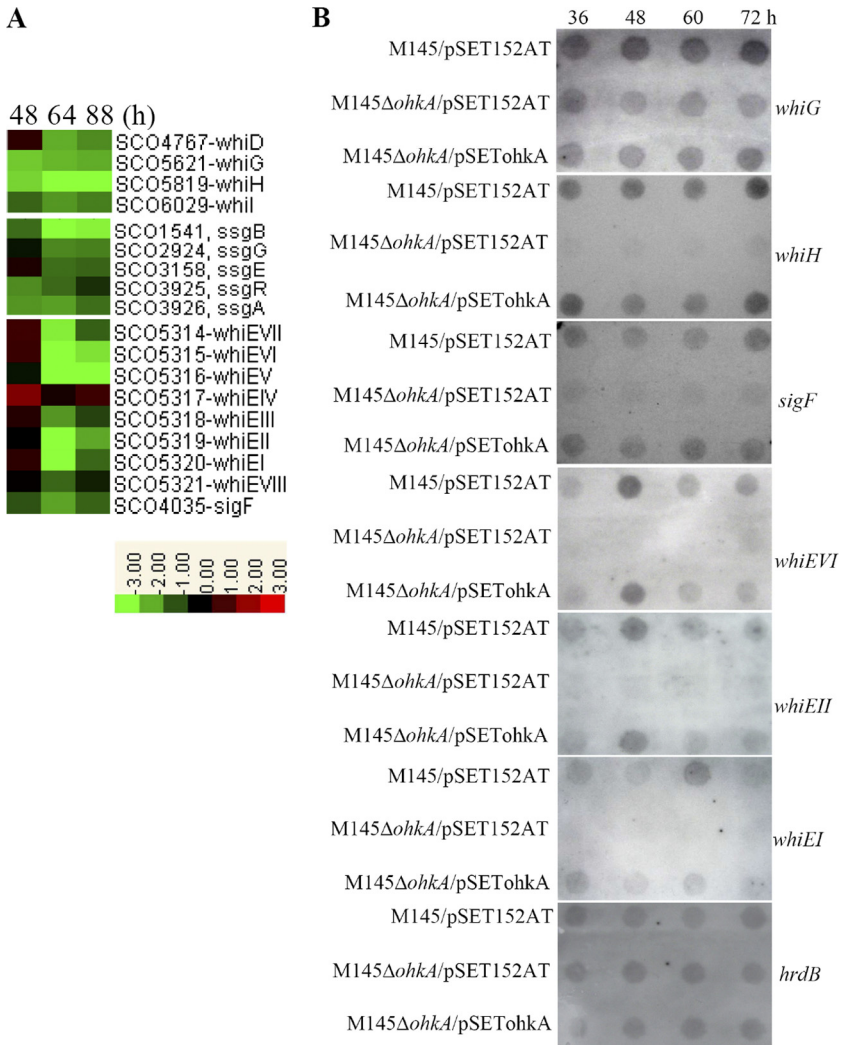

FIG. 5. Heat maps and RNA dot blot assays of selective gene clusters involved in spore formation and maturation in *S. coelicolor*. (A) Transcription profiles of genes associated with spore formation and maturation in the *ohkA* mutant, compared with M145. RNA samples from M145 and the *ohkA* mutant were isolated at the indicated time points on MS medium. The color representation is as described in the legend for Fig. 3. (B) RNA dot blot assay comparing the transcription of selected genes from panel A in M145/pSET152AT, M145Δ*ohkA*/pSET152AT, and M145Δ*ohkA*/pSETohkA. *hrdB* was used as a control for RNA loading levels.

molog; *cvnB* and *cvnC*, encoding two proteins of unknown function; and *cvnD*, encoding an ATP/GTP-binding protein (22). In some cases, the conserved operons are clustered with cytochrome P450 genes (31). Previous study has revealed the involvement of *cvn* genes in antibiotic production; inactivation of *cvnD9* in *S. coelicolor* resulted in overproduction of ACT and RED antibiotics (31). Interestingly, transcription of four conservons (*cvn*) (Fig. 6) was significantly reduced in the *ohkA* deletion mutant at three time points tested, which is confirmed by qRT-PCR (Table 2).

DNA microarray analysis also revealed that two important pleiotropic regulatory genes, *wblA* (SCO3579) (16, 24) and *nsdA* (SCO5582) (32), which regulate both antibiotic production and morphological differentiation, were downregulated in the mutant. The decreased expression of *wblA* transcription was further confirmed using qRT-PCR analysis (Table 2). In a later study of the *wblA* gene in *S. coelicolor* (16), the *wblA* mutant showed a similar phenotype as that of the *ohkA* mutant in this study, such as ACT overproduction, red colony color, and a higher biomass at late growth stage, etc. In addition, there is a significant overlap in the transcriptional profiles upon the respective deletion of *ohkA* and *wblA* (16). So we speculated that the effects of *ohkA* exerted on antibiotic biosynthesis and development might be partly mediated by the *wblA* gene, a theory which needs to be verified in the future.

Conclusions. In this study, we reported the characterization of a putative orphan histidine kinase, OhkA, and its roles in the regulation of both secondary metabolism and morphological differentiation in *S. coelicolor* and *S. avermitilis*. Genetic analysis showed that deletion of *ohkA* resulted in antibiotic overproduction and impaired aerial hypha and spore formation when strains were grown on MS agar. Disruption of the *ohkA* ortholog in *S. avermitilis* led to very similar effects as those of *ohkA* deletion in *S. coelicolor*, suggesting that this orphan HK

FIG. 6. Heat maps of four conservons in *S. coelicolor*. Transcription profiles of genes from four conservons in the *ohkA* mutant, compared with M145. RNA samples from M145 and the *ohkA* mutant were isolated at the indicated time points on MS medium. The color representation is as described in the legend for Fig. 3.

may represent a highly conserved signal transduction component among *Streptomyces* bacteria. Further transcription profile analysis revealed that OhkA played a global role in antibiotic biosynthesis, by influencing precursor supply, pleiotropic and pathway-specific antibiotic regulators and also some structural genes involved in cellular resistance to toxic effects. The effects of OhkA on development might be mediated through the functions of *bldN*/*M* (regulation of *chp* genes), *ramR*/*S* (SapB formation and regulation), *whiG*/*H*/*I* and *ssgA*/*R*/*G* (required for aerial hypha, septum, and spore formation), and *whiE* (spore maturation). Further studies are required (i) to determine what signal the orphan histidine kinase OhkA responds to and (ii) to identify the downstream paired response regulator of OhkA and then to fully understand the molecular mechanism underlying OhkA's effects on antibiotic biosynthesis and morphological differentiation in *S. coelicolor*.

ACKNOWLEDGMENTS

This work was supported by the National Natural Science Foundation of China (30770023, 30970033, and 30830002), the National Basic Research Program of China (2007CB707803 and 2011CBA00806), and the Special Program for Biological Sciences Research of the Chinese Academy of Sciences (KSCX2-EW-J-12) and the Natural Science Foundation of Shanghai (11ZR1442700).

We are grateful to Keith F. Chater for providing the PCR targeting system and Zhongjun Qin for providing the *S. coelicolor* and *S. avermitilis* cosmids.

REFERENCES

1. **Adamidis, T., P. Riggle, and W. Champness.** 1990. Mutations in a new *Streptomyces coelicolor* locus which globally block antibiotic biosynthesis but not sporulation. J. Bacteriol. **172:**2962–2969.
2. **Amon, J., et al.** 2008. Nitrogen control in *Mycobacterium smegmatis*: nitrogen-dependent expression of ammonium transport and assimilation proteins depends on the OmpR-type regulator GlnR. J. Bacteriol. **190:**7108–7116.
3. **Anderson, T. B., P. Brian, and W. C. Champness.** 2001. Genetic and transcriptional analysis of *absA*, an antibiotic gene cluster-linked two-component system that regulates multiple antibiotics in *Streptomyces coelicolor*. Mol. Microbiol. **39:**553–566.
4. **Bentley, S. D., et al.** 2002. Complete genome sequence of the model actinomycete *Streptomyces coelicolor* A3(2). Nature **417:**141–147.
5. **Bibb, M. J.** 2005. Regulation of secondary metabolism in streptomycetes. Curr. Opin. Microbiol. **8:**208–215.
6. **Brian, P., P. J. Riggle, R. A. Santos, and W. C. Champness.** 1996. Global negative regulation of *Streptomyces coelicolor* antibiotic synthesis mediated by an *absA*-encoded putative signal transduction system. J. Bacteriol. **178:**3221–3231.
7. **Capstick, D. S., J. M. Willey, M. J. Buttner, and M. A. Elliot.** 2007. SapB and the chaplins: connections between morphogenetic proteins in *Streptomyces coelicolor*. Mol. Microbiol. **64:**602–613.
8. **Chang, H. M., M. Y. Chen, Y. T. Shieh, M. J. Bibb, and C. W. Chen.** 1996. The *cutRS* signal transduction system of *Streptomyces lividans* represses the biosynthesis of the polyketide antibiotic actinorhodin. Mol. Microbiol. **21:**1075–1085.
9. **Chater, K. F.** 2001. Regulation of sporulation in *Streptomyces coelicolor* A3(2): a checkpoint multiplex? Curr. Opin. Microbiol. **4:**667–673.
10. **Chen, L., et al.** 2009. Transcriptomics analyses reveal global roles of the regulator AveI in *Streptomyces avermitilis*. FEMS Microbiol. Lett. **298:**199–207.
11. **Chen, L., et al.** 2008. Characterization of a negative regulator AveI for avermectin biosynthesis in *Streptomyces avermitilis* NRRL8165. Appl. Microbiol. Biotechnol. **80:**277–286.
12. **Claessen, D., et al.** 2004. The formation of the rodlet layer of streptomycetes is the result of the interplay between rodlins and chaplins. Mol. Microbiol. **53:**433–443.
13. **Datsenko, K. A., and B. L. Wanner.** 2000. One-step inactivation of chromosomal genes in *Escherichia coli* K-12 using PCR products. Proc. Natl. Acad. Sci. U. S. A. **97:**6640–6645.
14. **Elliot, M. A., et al.** 2003. The chaplins: a family of hydrophobic cell-surface proteins involved in aerial mycelium formation in *Streptomyces coelicolor*. Genes Dev. **17:**1727–1740.
15. **Flardh, K., and M. J. Buttner.** 2009. *Streptomyces* morphogenetics: dissecting differentiation in a filamentous bacterium. Nat. Rev. Microbiol. **7:**36–49.
16. **Fowler-Goldsworthy, K., et al.** 2011. The actinobacteria-specific gene *wblA* controls major developmental transitions in *Streptomyces coelicolor* A3(2). Microbiology doi:10.1099/mic.0.047555-0.
17. **Gottelt, M., S. Kol, J. P. Gomez-Escribano, M. Bibb, and E. Takano.** 2010. Deletion of a regulatory gene within the *cpk* gene cluster reveals novel antibacterial activity in *Streptomyces coelicolor* A3(2). Microbiology **156:**2343–2353.
18. **Gust, B., G. L. Challis, K. Fowler, T. Kieser, and K. F. Chater.** 2003. PCR-targeted *Streptomyces* gene replacement identifies a protein domain needed for biosynthesis of the sesquiterpene soil odor geosmin. Proc. Natl. Acad. Sci. U. S. A. **100:**1541–1546.
19. **Guthrie, E. P., et al.** 1998. A response-regulator-like activator of antibiotic synthesis from *Streptomyces coelicolor* A3(2) with an amino-terminal domain that lacks a phosphorylation pocket. Microbiology **144:**727–738.
20. **Hopwood, D. A.** 1999. Forty years of genetics with *Streptomyces*: from *in vivo* through *in vitro* to *in silico*. Microbiology **145:**2183–2202.
21. **Huang, J., et al.** 2005. Cross-regulation among disparate antibiotic biosynthetic pathways of *Streptomyces coelicolor*. Mol. Microbiol. **58:**1276–1287.
22. **Hutchings, M. I., P. A. Hoskisson, G. Chandra, and M. J. Buttner.** 2004. Sensing and responding to diverse extracellular signals? Analysis of the sensor kinases and response regulators of *Streptomyces coelicolor* A3(2). Microbiology **150:**2795–2806.
23. **Ishizuka, H., S. Horinouchi, H. M. Kieser, D. A. Hopwood, and T. Beppu.** 1992. A putative two-component regulatory system involved in secondary metabolism in *Streptomyces* spp. J. Bacteriol. **174:**7585–7594.
24. **Kang, S. H., et al.** 2007. Interspecies DNA microarray analysis identifies WblA as a pleiotropic down-regulator of antibiotic biosynthesis in *Streptomyces*. J. Bacteriol. **189:**4315–4319.
25. **Kanth, B. K., H. N. Jnawali, N. P. Niraula, and J. K. Sohng.** 2010. Superoxide dismutase (SOD) genes in *Streptomyces peucetius*: effects of SODs on secondary metabolites production. Microbiol. Res. doi:10.1016/j.micres.2010.07.003.
26. **Keijser, B. J., G. P. van Wezel, G. W. Canters, and E. Vijgenboom.** 2002. Developmental regulation of the *Streptomyces lividans ram* genes: involvement of RamR in regulation of the *ramCSAB* operon. J. Bacteriol. **184:**4420–4429.
27. **Kelemen, G. H., et al.** 1998. Developmental regulation of transcription of *whiE*, a locus specifying the polyketide spore pigment in *Streptomyces coelicolor* A3(2). J. Bacteriol. **180:**2515–2521.
28. **Kelemen, G. H., et al.** 1996. The positions of the sigma-factor genes, *whiG* and *sigF*, in the hierarchy controlling the development of spore chains in the aerial hyphae of *Streptomyces coelicolor* A3(2). Mol. Microbiol. **21:**593–603.
29. **Kieser, T., M. Bibb, M. Buttner, and K. Chater.** 2000. Practical *Streptomyces* genetics. John Innes Foundation, Norwich, England.
30. **Kirby, R., and D. A. Hopwood.** 1977. Genetic determination of methyleno-

mycin synthesis by the SCP1 plasmid of *Streptomyces coelicolor* A3(2). J. Gen. Microbiol. **98:**239–252.
31. **Komatsu, M., et al.** 2006. Proteins encoded by the conservon of *Streptomyces coelicolor* A3(2) comprise a membrane-associated hetero-complex that resembles eukaryotic G protein-coupled regulatory system. Mol. Microbiol. **62:**1534–1546.
32. **Li, W., et al.** 2006. Identification of a gene negatively affecting antibiotic production and morphological differentiation in *Streptomyces coelicolor* A3(2). J. Bacteriol. **188:**8368–8375.
33. **Li, Y. Q., P. L. Chen, S. F. Chen, D. Wu, and J. Zheng.** 2004. A pair of two-component regulatory genes *ecrA1*/*A2* in *Streptomyces coelicolor*. J. Zhejiang Univ. Sci. **5:**173–179.
34. **Lu, Y., et al.** 2007. Characterization of a novel two-component regulatory system involved in the regulation of both actinorhodin and a type I polyketide in *Streptomyces coelicolor*. Appl. Microbiol. Biotechnol. **77:**625–635.
35. **MacNeil, D. J., et al.** 1992. Analysis of *Streptomyces avermitilis* genes required for avermectin biosynthesis utilizing a novel integration vector. Gene **111:** 61–68.
36. **Mascher, T., J. D. Helmann, and G. Unden.** 2006. Stimulus perception in bacterial signal-transducing histidine kinases. Microbiol. Mol. Biol. Rev. **70:**910–938.
37. **Nguyen, K. T., et al.** 2002. A central regulator of morphological differentiation in the multicellular bacterium *Streptomyces coelicolor*. Mol. Microbiol. **46:**1223–1238.
38. **Noens, E. E., et al.** 2005. SsgA-like proteins determine the fate of peptidoglycan during sporulation of *Streptomyces coelicolor*. Mol. Microbiol. **58:** 929–944.
39. **Pawlik, K., M. Kotowska, and P. Kolesinski.** 2010. *Streptomyces coelicolor* A3(2) produces a new yellow pigment associated with the polyketide synthase Cpk. J. Mol. Microbiol. Biotechnol. **19:**147–151.
40. **Ryding, N. J., T. B. Anderson, and W. C. Champness.** 2002. Regulation of the *Streptomyces coelicolor* calcium-dependent antibiotic by *absA*, encoding a cluster-linked two-component system. J. Bacteriol. **184:**794–805.
41. **Ryu, Y. G., M. J. Butler, K. F. Chater, and K. J. Lee.** 2006. Engineering of primary carbohydrate metabolism for increased production of actinorhodin in *Streptomyces coelicolor*. Appl. Environ. Microbiol. **72:**7132–7139.
42. **Sambrook, J., E. F. Fritsch, and T. Maniatis.** 1989. Molecular cloning: a laboratory manual, 2nd ed. Cold Spring Harbor Laboratory Press, Cold Spring Harbor, NY.
43. **San Paolo, S., J. Huang, S. N. Cohen, and C. J. Thompson.** 2006. *rag* genes: novel components of the RamR regulon that trigger morphological differentiation in *Streptomyces coelicolor*. Mol. Microbiol. **61:**1167–1186.
44. **Shu, D., et al.** 2009. *afsQ1-Q2-sigQ* is a pleiotropic but conditionally required signal transduction system for both secondary metabolism and morphological development in *Streptomyces coelicolor*. Appl. Microbiol. Biotechnol. **81:**1149–1160.
45. **Sola-Landa, A., R. S. Moura, and J. F. Martin.** 2003. The two-component PhoR-PhoP system controls both primary metabolism and secondary metabolite biosynthesis in *Streptomyces lividans*. Proc. Natl. Acad. Sci. U. S. A. **100:**6133–6138.
46. **Stock, A. M., V. L. Robinson, and P. N. Goudreau.** 2000. Two-component signal transduction. Annu. Rev. Biochem. **69:**183–215.
47. **Takano, E., et al.** 2005. A bacterial hormone (the SCB1) directly controls the expression of a pathway-specific regulatory gene in the cryptic type I polyketide biosynthetic gene cluster of *Streptomyces coelicolor*. Mol. Microbiol. **56:**465–479.
48. **Taylor, B. L., and I. B. Zhulin.** 1999. PAS domains: internal sensors of oxygen, redox potential, and light. Microbiol. Mol. Biol. Rev. **63:**479–506.
49. **Tian, Y., K. Fowler, K. Findlay, H. Tan, and K. F. Chater.** 2007. An unusual response regulator influences sporulation at early and late stages in *Streptomyces coelicolor*. J. Bacteriol. **189:**2873–2885.
50. **Traag, B. A., G. H. Kelemen, and G. P. Van Wezel.** 2004. Transcription of the sporulation gene *ssgA* is activated by the IclR-type regulator SsgR in a *whi*-independent manner in *Streptomyces coelicolor* A3(2). Mol. Microbiol. **53:**985–1000.
51. **van Wezel, G. P., et al.** 2000. *ssgA* is essential for sporulation of *Streptomyces coelicolor* A3(2) and affects hyphal development by stimulating septum formation. J. Bacteriol. **182:**5653–5662.
52. **Wilkinson, C. J., et al.** 2002. Increasing the efficiency of heterologous promoters in actinomycetes. J. Mol. Microbiol. Biotechnol. **4:**417–426.
53. **Willemse, J., J. W. Borst, E. de Waal, T. Bisseling, and G. P. van Wezel.** 2011. Positive control of cell division: FtsZ is recruited by SsgB during sporulation of *Streptomyces*. Genes Dev. **25:**89–99.
54. **Willey, J., R. Santamaria, J. Guijarro, M. Geistlich, and R. Losick.** 1991. Extracellular complementation of a developmental mutation implicates a small sporulation protein in aerial mycelium formation by *Streptomyces coelicolor*. Cell **65:**641–650.
55. **Wu, G., D. E. Culley, and W. Zhang.** 2005. Predicted highly expressed genes in the genomes of *Streptomyces coelicolor* and *Streptomyces avermitilis* and the implications for their metabolism. Microbiology **151:**2175–2187.
56. **Yu, T. W., and D. A. Hopwood.** 1995. Ectopic expression of the *Streptomyces coelicolor whiE* genes for polyketide spore pigment synthesis and their interaction with the act genes for actinorhodin biosynthesis. Microbiology **141:**2779–2791.
57. **Zhang, W., and L. Shi.** 2005. Distribution and evolution of multiple-step phosphorelay in prokaryotes: lateral domain recruitment involved in the formation of hybrid-type histidine kinases. Microbiology **151:**2159–2173.
58. **Zhao, B., et al.** 2008. Biosynthesis of the sesquiterpene antibiotic albaflavenone in *Streptomyces coelicolor* A3(2). J. Biol. Chem. **283:**8183–8189.